Synthesis and Characterization of Bead-like Poly(N-isopropylacrylamide) Copolymers with Double Decker Silsesquioxanes in the Main Chains

Journal:	*Polymer Chemistry*
Manuscript ID:	PY-ART-06-2014-000786.R1
Article Type:	Paper
Date Submitted by the Author:	25-Jul-2014
Complete List of Authors:	Wei, Kun; Shanghai Jiao Tong Univeristy, Department of Polymer Science and Engineering Wang, Lei; Shanghai Jiao Tong Univeristy, Department of Polymer Science and Engineering Li, Lei; Shanghai Jiao Tong Univeristy, Department of Polymer Science and Engineering Zheng, Sixun; Shanghai Jiao Tong Univeristy, Department of Polymer Science and Engineering

Synthesis and Characterization of Bead-like Poly(N-isopropylacrylamide) Copolymers with Double Decker Silsesquioxane in the Main Chains

Kun Wei, Lei Wang, Lei Li and Sixun Zheng*

Department of Polymer Science and Engineering and the State Key Laboratory of Metal Matrix Composites, Shanghai Jiao Tong University, Shanghai 200240, P. R. China

* To whom correspondence should be addressed. Email: *szheng@sjtu.edu.cn (S. Zheng)*; Tel: 86-21-54743278; Fax: 86-21-54741297.

ABSTRACT

Bead-like PNIPAAm copolymers with double-decker silsesquioxane (DDSQ) in the main chains were synthesized *via* reversible addition-fragmentation chain transfer polymerization (RAFT) approach. The macromolecular chain transfer agent used for the RAFT polymerization was synthesized *via* the polycondensation of 3,13-dihydroxypropyloctaphenyl DDSQ with *S,S'*-bis(α,α'-dimethyl-α''-propargyl acetate)trithiocarbonate. The organic-inorganic copolymers with variable contents of DDSQ were characterized by means of ^{1}H nuclear magnetic resonance spectroscopy and gel permeation chromatography. Transmission electron microscopy showed that the bead-like PNIPAAm copolymers were microphase-separated in bulks. It was found that the glass transition temperatures (T_g's) of PNIPAAm microdomains of the organic-inorganic copolymers were lower than plain PNIPAAm and decreased with increasing the content of DDSQ. The bead-like PNIPAAm copolymers displayed the self-assembly behavior in aqueous solutions. Depending on the content of DDSQ, the bead-like organic-inorganic copolymers can self-assemble into spherical or vesicular self-assembled nanoobjects in aqueous solutions. Both micro-differential scanning calorimetry (Micro-DSC) and cloud point analysis with UV-vis spectroscopy showed that lower critical solution temperature (LCST) behavior of PNIPAAm subchains in the bead-like copolymers was significantly affected by the POSS cages in the main chains.

(**Keywords:** polyhedral oligomeric silsesquioxane; poly(N-isopropylacrylamide), RAFT Polymerization; organic-inorganic hybrid copolymers)

INTRODUCTION

Polyhedral oligomeric silsesquioxanes (POSS) are known as a class of important building blocks for organic-inorganic hybrids[1-6]. The POSS-containing polymers can display excellent comprehensive properties *via* the synergism of POSS and organic polymers. A typical POSS molecule is composed of a cage-like Si-O framework and several organic groups, each of which is covalently bonded to one Si atom. Depending on the type and number of functional groups, the POSS macromers can be incorporated into organic polymers to obtain the organic-inorganic nanocomposites with various approaches[2-6]. For instance, the POSS macromers bearing single polymerizable groups can be directly copolymerized with monomers of organic polymers and those containing other single reactive groups can be incorporated into organic polymers *via* reactive blending approach. In addition, monofunctional POSS macromers can be bonded to the ends of polymer chains to form so-called POSS-capped telechelics[7-14]. In these organic-inorganic hybrids, POSS cages behave as either pendent side groups or end groups and the main chains of polymers remain unchanged. For multi-functional POSS macromers, the organic-inorganic nanocomposites can be prepared *via* crosslinking copolymerization approach[15-29]. In ample literature, the POSS-containing thermosetting polymers such as polyimide[17], polyurethane[18-20], poly(methyl methacrylate)[21], polybenzoxazines[28,29] and poly(ethylene imine)[30] have been prepared by the use of octafunctional POSS macromers. In this class of organic-inorganic hybrids, POSS cages were built into the crosslinked networks in the form of the nanosized crosslinkers.

Compared to the above POSS-containing polymers, linear organic-inorganic polymers with POSS in the main chains (*i.e.*, so-called bead-like copolymers) are attractive. On the one hand, the thermomechanical properties of the polymers can be improved with the interlay of the cage-like building blocks (*i.e.,* POSS) in the main chains. On the other hand, this class of organic-inorganic hybrids could possess the simplicity in the materials processing as thermoplastics owing to their linear chain structures. To prepare this class of organic-inorganic polymers, it is prerequisite to use well-defined difunctional POSS macromers. Nonetheless, such a study remains largely unexplored because efficient synthesis of well-defined difunctional POSS macromers is still a challenging task. Wright and Feher *et al.*[31] first reported the synthesis of a difunctional POSS macromer bearing two aminophenyl groups *via*

multi-step reactions. This POSS diamine was used to synthesize the linear polyimide hybrids with the POSS in the main chains. By controlling the molar ratio of the POSS macromer to other low-molecule diamines [*viz.* 1,3-bis(3-aminophenoxy)benzene and/or 3,4'-oxydianiline], the polyimide hybrids were obtained with variable contents of POSS. By using a double-decker silsesquioxane (DDSQ) bearing two aminophenyl groups, Kakimoto *et al.* also synthesized the organic-inorganic polyimides with POSS in the main chains[32-34]. It was found that the polyimide hybrids exhibited the improved thermomechanical and dielectric properties. By using the cross-dehydrocoupling polycondensation of DDSQ with octamethyltetrasiloxane, Kawakami *et al.*[35] incorporated DDSQ into the main chains of polysiloxanes. It was found that the modified polysiloxanes exhibited good transparency with low cutoff wavelength and outstanding thermal stability. More recently, Zheng and coworkers[36-38] reported the syntheses of several novel linear organic-inorganic polymers with DDSQ in the main chains, such as poly(hydroxyether of bisphenol A) and polyurethane. It was found that that the presence of even a small amount of POSS can result in a significant improvement in thermomechanical properties of materials. In all these previous works, only step-growth polymerizations involving condensation[31-34] and addition[36-38] including the copper-catalyzed Huisgen 1,3-dipolar cycloaddition[38] were utilized to obtain the organic-inorganic copolymers with POSS in the main chains. To the best of our knowledge, there has been no previous report on the synthesis of linear hybrid copolymers with POSS in the main chains *via* a controlled/living radical polymerization approach.

Poly(N-isopropylacrylamide) (PNIPAAm) is an interesting thermoresponsive polymer. In aqueous solution it displays a lower critical solution temperature (LCST) behavior at *c.a.* 32 °C [39-43]. Below this temperature, individual PNIPAAm chains adopt a random coil conformation. It is proposed that there are the intermolecular hydrogen bonding interactions between amide groups of PNIPAAm and water, which promote the solubility of this polymer with water. Upon heating up to 32 °C or higher, the random coils will collapse into globules. Under this circumstance, the intermolecular hydrogen bonding interactions are interrupted owing to the conformational changes of PNIPAAm. As a consequence, the hydrophobic association among the collapsed PNIPAAm chains occurs and the polymer chains become water-insoluble. The thermoresponsive behavior of PNIPAAm endows this polymer

with potential applications in biomedical and biochemical fields such as drug delivery and protein separation[44-47]. In the past years, the LCST behaviors of PNIPAAm in aqueous solutions have been extensively studied[40-43, 48-54]. It has been realized that several structural factors such as co-monomer, tacticity, crosslinking, grafting, topology of macromolecules, molecular weights and end groups all affect the LCST behavior of PNIPAAm[55-61]. Recently, the PNIPAAm hybrids containing POSS have attracted considerable interest since the inclusion of POSS can significantly affect the LCST behaviors of PNIPAAm[40,62,63]. In all previous PNIPAAm hybrids investigated, POSS macromers have been either grafted onto PNIPAAm chains or capped to ends of PNIPAAm chains and the main chains of PNIPAAm remained unchanged. To the best of our knowledge, there has been no precedent report on the incorporation of POSS in the main chains of PNIPAAm.

In this work, we explored to synthesize a novel PNIPAAm hybrid with POSS in the main chains *via* reversible addition-fragmentation chain transfer polymerization (RAFT) approach. The macromolecular chain transfer agent (Macro-CTA) used for the RAFT polymerization was a bead-like polymer with DDSQ in the main chain. This bead-like polymer also contained trithiocarbonate structural units in its main chain. The Macro-CTA was synthesized *via* the polycondensation of 3,13-dihydroxypropyloctaphenyl DDSQ with *S,S'*-bis(α,α'-dimethyl-α"-propargylacetate)trithiocarbonate (BDPT). The purpose of this work is twofold: i) to explore the synthesis of the bead-like copolymers with POSS in the main chain *via* living radical polymerization approach and ii) to investigate the effect of POSS in the main chains on thermoresponsive properties of PNIPAAm. The bead-like PNIPAAm copolymers would be characterized by means of nuclear magnetic resonance spectroscopy (NMR) and gel permeation chromatography (GPC). The self-assembly and thermoresponsive behavior of the bead-like PNIPAAm copolymers were investigated by means of differential scanning calorimetry (DSC), transmission electron microscopy (TEM), dynamic laser scattering (DLS) and cloud point analysis with UV-vis spectroscopy.

EXPERIMENTAL

Materials

Phenyltrimethoxysilane (98%) was obtained from Zhejiang Chemical Technology Co., China. Other organosilanes such as methyldichlorosilane and allyloxytrimethylsilane were purchased form Aldrich Co., USA and used as received. Karstedt catalyst (*viz.* the complex of Platinum with divinyltetramethyldisiloxane (DVS) dissolved in toluene at the concentration of 2 wt%) was purchased from Aldrich Co., USA. N-isopropylacrylamide (NIPAAm) was prepared in this lab. N-(3-dimethylaminopropyl)-N'-ethylcarbodiimide 2,2'-azobisisobutylnitrile, hydrochloride, 4-dimethylaminopyridine, calcium hydride (CaH_2), sodium hydroxide (NaOH) and carbon disulfide (CS_2) were supplied by Shanghai Reagent Co., China. Organic solvents such as toluene, tetrahydrofuran, isopropyl alcohol, triethylamine, methanol, N,N'-dimethylformamide and chloroform were of chemically pure grade, obtained from commercial sources. Before use, toluene and tetrahydrofuran were refluxed above metal sodium and then distilled and stored in the presence of a molecular sieve of 4Å; triethylamine was refluxed over CaH_2 and then was treated with *p*-toluenesulfonyl chloride, followed by distillation.

Synthesis of 3,13-Dihydro DDSQ

First, octaphenyldicycloocatasiloxane tetrasodium silanolate [$Na_4O_{14}Si_8(C_6H_5)_8$] was synthesized by following the method of literature reported by Kakimoto *et al.* [64] with slight modification. Typically, phenyltrimethoxysilane (71.380 g, 0.36 mol), isopropyl alcohol (360 ml), deionized water (7.450 g, 0.41 mol) and sodium hydroxide (9.50g, 0.24mol) were charged to a flask equipped with a condenser and a magnetic stirrer. After refluxed for 4 hours, the reactive system was cooled down to room temperature with vigorous stirring for additional 15 hours. All the solvent and other volatile were removed *via* rotary evaporation and the white solids were obtained. After dried at 60 ^oC *in vacuo* for 12 hours, the product (82.570 g) was obtained with the yield of 85%.

Second, the silylation reaction between $Na_4O_{14}Si_8(C_6H_5)_8$ and methyldichlorosilane was carried out to prepare 3,13-dihydrooctaphenylhexacyclodecasiloxane (denoted dihydro DDSQ). Typically, $Na_4O_{14}Si_8(C_6H_5)_8$ (34.800 g, 30.0 mmol) and triethylamine (12.5 mL, 123.6mmol) were charged to a flask equipped with a magnetic stirrer, 300 mL of anhydrous

tetrahydrofuran were added with vigorous stirring. The flask was immersed into an ice-water bath and purged with highly pure nitrogen for one hour. After that, methyldichlorosilane (10.350 g, 90.0 mmol) dissolved in 30 mL tetrahydrofuran were added dropwise within 30 min. The reaction was performed at 0 ^{o}C for 4 hours and at room temperature for 20 hours. The insoluable solids (*i.e.*, sodium chloride and unreacted tetrasodium silanolate) were removed by centrifuge and the solvents together with other volatile compounds were eliminated *via* rotary evaporation to afford the white solids. The solids were washed with 300 mL of methanol thrice and dried *in vacuo* at 40 ^{o}C for 24 hours; the product (14.900 g) was obtained with the yield of 43%. ^{1}H NMR (ppm, $CDCl_3$): 0.38 (*d*, 6.0H, C***H*$_3$**Si), 4.98 (*d*, 2.0H, Si***H***), 7.14 ~ 7.50 (*m*, 40H, protons of aromatic rings); ^{29}Si NMR (ppm, $CDCl_3$): -32.72, -77.73, -79.02, -79.21 and -79.42.

Synthesis 3,13-Di(trimethylsilyl)oxypropyl DDSQ

To a flask equipped with a magnetic stirrer, 3,13-dihydro DDSQ (10.880 g, 4.70 mmol), anhydrous toluene (50 mL) and allyloxytrimethylsilane (13.000 g, 102.4 mmol) were charged. The flask was connected to a Schlenk line to degas with a repeated exhausting-refilling process with highly pure nitrogen and then Karstedt catalyst was added with vigorous stirring. The hydrosilylation was performed at 95 ^{o}C for 36 hours to ensure that the reaction went to completion. The solvent and excess allyloxytrimethylsilane were removed *via* rotary evaporation to afford the solids with the yield of 98 %. ^{1}H NMR (ppm, $CDCl_3$): 0.00 [*s*, 8.8H, -OSiCH_3 and $CH_2CH_2CH_2OSi(C\boldsymbol{H_3})_3$], 0.30 [*s*, 3.22H, -OSiC***H*$_3$**$CH_2CH_2CH_2OSi(CH_3)_3$], 0.71 [*t*, 2.1H, -OSiCH_3C***H*$_2$**$CH_2CH_2OSi(CH_3)_3$], 1.62 [*m*, 2.1H, -OSiCH_3CH_2C***H*$_2$**$CH_2OSi(CH_3)_3$] and 3.44 [*t*, 2.0H, -OSiCH_3CH_2 CH_2C***H*$_2$**$OSi(CH_3)_3$].

Synthesis of 3,13-Dihydroxypropyl DDSQ

To a flask equipped with a magnetic stirrer, 3,13-di(trimethylsilyl)oxypropyl DDSQ (6.000 g, 4.240 mmol) and dichloromethane (90 ml) were charge and then 90 mL of methanol was added with vigorous stirring. Thereafter, methyltrichlorosilane (1.360 g, 12.52 mmol) was dropwise added using a syringe within 30 min. The

reaction was performed at room temperature for 5 hours. The solvents and the excess methyltrichorosilane were removed *via* rotary evaporation. The resulting product was obtained *via* recrystallization from the mixture of THF with hexane (50/50 vol). After dried in a vacuum oven at 40 °C for 24 hours, the product (4.710 g) was obtained with the yield of 87 %. ^{1}H NMR (ppm, $CDCl_3$): 0.31 (*s*, 3.1H, -OSiC***H*****$_3$**$CH_2CH_2CH_2OH$), 0.74 [*t*, 2.0H, -$OSiCH_3C$***H*****$_2$**CH_2CH_2OH], 1.63 [*m*, 2.2H, -$OSiCH_3CH_2C$***H*****$_2$**CH_2OH], 3.47 [*t*, 2.0H, $OSiCH_3CH_2CH_2C$***H*****$_2$**OH]; MALDI-TOF-Mass (Product + Na^+): 1292.1Da (Calculated: 1291.9 Da).

Synthesis of S,S'-Bis(α,α'-dimethyl-α''-propargyl acetate)trithiocarbonate

S,S'-bis(*α,α*'-dimethyl-*α*''-aceticacid)trithiocarbonate (BDATC) was synthesized by following the method of literature[65-68]. Typically, to a flask equipped with a mechanical stirring, carbon disulfide (6.850 g, 0.09 mol), chloroform (26.875 g, 0.225 mol), acetone (13.075 g, 0.225 mol), tetrabutylammonium bromide (0.572 g, 1.775 mmol) and 30 ml mineral spirits were charged with vigorous stirring. At 0 °C, this flask was purged with highly pure nitrogen and the aqueous solution of sodium hydroxide (50%) (50.500 g, 0.63 mol) was slowly dropped within 30 min. This reacrtion was performed at 25 °C for 12 hours and then 225 mL of deionized water was added to dissolve the solids, followed by adding 30 mL of hydrochoric acid (37%) to acidify the aqueous layer. With vigorous stirring for additional 30 min, the earth-colored insoluable solids was filtered out and washed with water thrice. The crude product was collected after drying *in vacuo* at 40 °C overnight. After recrystallization in the mixture of toluene with acetone (4/1 volume), the product (13.200g) was obtained with the yiled of 65%. ^{1}H NMR (ppm, $CDCl_3$): 1.69 [*s*, -$CSSC(CH_3)_2COO$], ^{13}C NMR (ppm, DMSO-d_6): 25.6 [-$CSSC(CH_3)_2COO$], 56.8 [-$CSSC(CH_3)_2COO$], 173.7 [-$CSSC(CH_3)_2COO$], 219.8 [-$CSSC(CH_3)_2COO$].

Synthesis of Macromolecular Chain Transfer Agent (DDSQ-CTA)

To a flask equipped with a magnetic stirrer, 3,13-dihydroxypropyl DDSQ (2.550 g, 2.0 mmol), BDTAC (0.560 g, 2.0 mmol), EDC (0.770 g, 4.0 mmol) and DMAP (0.150 g, 1.2 mmol) were charged and then 100 mL of dichloromethane was

added. Under a nitrogen atmosphere, the reaction was carried out at room temperature for 36 hours. After that, the insoluble solids were filtered out and the remaining solution was concentrated *via* rotary evaporation. The solution was dropped into 50 mL of hexane to afford the precipitates. After dried *in vacuo* at room temperature for 24 hours, the product (2.310 g) was obtained with the yield of 76%. ^{1}H NMR (ppm, $CDCl_3$): 1.55 [*s*, $C(C\boldsymbol{H_3})_2COOCH_2$], 0.30 (*s*, -$OSiC\boldsymbol{H_3}CH_2CH_2CH_2OOC$), 0.71 [*t*, -$OSiCH_3C\boldsymbol{H_2}CH_2CH_2OOC$], 1.65 [*m*, -$OSiCH_3CH_2C\boldsymbol{H_2}CH_2OOC$], 3.95 [*t*, $OSiCH_3CH_2CH_2C\boldsymbol{H_2}OOC$]. GPC (PS standard, DMF): M_n=7,700 Da with M_w/M_n=1.74.

Synthesis of Bead-like PNIPAAm Copolymers with DDSQ in the Main Chains

The above DDSQ-CTA was used to synthesize bead-like PNIPAAm copolymers with DDSQ in the main chains *via* reversible addition fragmentation chain transfer (RAFT) polymerization. Typically, to a flask equipped with a magnetic stirrer, NIPAAm (0.350 g, 3.09 mmol), DDSQ-CTA (0.150g, 0.10 mmol) and AIBN (4.20 mg, 0.026 mmol) were charged and then 2 mL of 1,4-dioxane was added. The flask was connected onto a Schenk line and three freeze-evacuate-thaw cycles were used to remove a trace of oxygen. The polymerization was performed at 60 ^{o}C for 20 hours. The reacted mixture was dropped into 50 mL of cold diethyl ether to afford the precipitates. The precipitates was re-dissolved in 1,4-dioxane and the solution was re-dropped into cold diethyl ether to obtain the precipitates; this procedure was repeated thrice to purify the polymer. After dried *in vacuo* at 25 ^{o}C for 24 hours, the product (0.380g) was obtained with the conversion of the monomer to 76%. GPC: M_n =55,100 Da with M_w/M_n =1.58.

Measurement and Techniques

Nuclear Magnetic Resonance Spectroscopy (NMR)

The ^{1}H NMR measurements were carried out on a Varian Mercury Plus 400 MHz NMR spectrometer at 25 ^{o}C and the ^{29}Si NMR spectra were obtained on a Bruker Avance III 400 MHz NMR spectrometer. The samples were dissolved with deuterium chloroform ($CDCl_3$) and the solutions were measured with

tetramethylsilane (TMS) as an internal reference.

Matrix-Assisted Ultraviolet Laser Desorption / Ionization Time-of-Flight Mass Spectroscopy (MALDI-TOF-MS)

The MALDI-TOF-MS experiment was carried out on an IonSpec HiResMALDI mass spectrometer equipped with a pulsed nitrogen laser (λ = 337 nm; pulse with = 3 ns). This instrument operated at an accelerating potential of 20 kV in reflector mode. Sodium is used as the cationizing agent and all the data shown are for positive ions. Gentisic acid (2,5-dihydroxybenzoic acid, DHB) was used as the matrix with dichloromethane as the solvent.

Gel Permeation Chromatography (GPC)

The molecular weights and molecular weight distribution of polymers were determined on a Waters 717 Plus autosampler gel permeation chromatography apparatus equipped with Waters RH columns and a Dawn Eos (Wyatt Technology) multi-angle laser light scattering detector and the measurements were carried out at 25 ^{o}C with N,N'-dimethylformamide (DMF) as the eluent at the rate of 1.0 mL/min.

Differential Scanning Calorimetry (DSC)

The calorimetric measurements were performed on a TA Instruments Q2000 differential scanning calorimeter in dry nitrogen atmosphere. The instrument was calibrated with a standard indium. In order to measure glass transition temperature (T_g) a heating rate 20 ^{o}C /min was used in all cases. Glass transition temperature (T_g) was taken as the midpoint of the heat capacity change.

Micro-Differential Scanning Calorimetry (Micro-DSC)

The specimens for Micro-DSC measurements were prepared by dissolving the hybrid copolymers in highly pure water at the concentration of *c.a.* 30 mg/mL. The

Micro-DSC measurements were performed with a SETARAM III Micro-DSC under a dry nitrogen atmosphere and circulating water. Before the measurement, the solution samples (*c.a.* 0.6 mL) were maintained at 18 ^{o}C for 15 min and then heated up to 60 ^{o}C at the heating rate of 1 ^{o}C/min. The position of the maximum of exothermic peak was taken as the lower critical solution temperature (LCST).

Determination of Cloud Points

Typically, a bead-like PNIPAAm copolymer with DDSQ in the main chains (0.01 g) was dissolved in the 0.5 mL of THF and then 50 mL of ultrapure water was dropwise added by a dropping funnel. With vigorous stirring for additional 30 min, a transparent suspension was obtained with the concentration of 0.02 wt%. The solvent (*i.e.,* THF) in the suspension was eliminated *via* rotary evaporation at 60 ^{o}C. The cloud points were determined with an Agilent Technologies Cary 60 Ultraviolet-visible spectrometer at the wavelength of light to be λ = 550 nm. A thermostatically controlled cuvette holder was employed and the plots of light transmittance as a function of temperature were obtained.

Dynamic Laser Scattering (DLS)

The aqueous solutions of polymers (10.0 mg) dissolved in 0.5 mL of tetrahydrofuran was charged to a flask containing 50 mL of ultra-pure water with a dropping funnel with vigorous stirring. The solutions were dialyzed in ultrapure water for 3 days prior to the measurements. The laser light scattering experiments were conducted on a Malvern Nano ZS90 equipped with a He-Ne laser operated at the wavelength of λ = 633 nm and the data were collected at a fixed scattering angle of 90^{o}.

Transmission Electron Microscopy (TEM)

The morphological observations were conducted on a JEOL JEM 2100F transmission electron microscope at a voltage of 200 kV. To investigate the morphology of the samples in bulks, the THF solutions of the polymers at the

concentration of 1 wt% were cast on carbon-coated copper grids and the solvent was slowly evaporated at room temperature and then *in vacuo* at 30 ^{o}C for 2 hours. The specimens were directly observed without an additional staining step. To investigate the self-assembly behavior of the samples in aqueous solutions, the specimens were prepared by dropping the suspensions of the polymer in water (about 10 μl at 0.2 g × L^{-1}) onto carbon-coated copper grids; the water was eliminated *via* freeze-drying approach.

RESULTS AND DISCUSSION

Synthesis of DDSQ-CTA

The route of synthesis for the DDSQ-CTA was shown in Schemes 1 and 2. First, 3,13-dihydroxypropyl DDSQ was synthesized as detailed in a previous work[37] Herewith, the route of the synthesis was described in brief. Octaphenyldicycloocatasiloxane tetrasodium silanolate [$Na_4O_{14}Si_8(C_6H_5)_8$] was synthesized by following the method of the literature reported by Kakimoto *et al.*[64] The silylation reaction between $Na_4O_{14}Si_8(C_6H_5)_8$ and methyldichlorosilane was carried out to afford 3,13-dihydro DDSQ. The hydrosilylation reaction between 3,13-dihydro DDSQ and allyloxytrimethylsilane was performed to afford 3,13-di(trimethylsilyl)oxypropyl DDSQ. The deprotection reaction of 3,13-di(trimethylsilyl)oxypropyl DDSQ *via* hydrolysis was carried out to afford 3,13-dihydroxypropyl DDSQ. The results of ^{1}H and ^{29}Si NMR and MALDI-TOF mass spectroscopy indicate that the difunctional POSS macromer was successfully obtained[36-38]. Second, the polycondensation of 3,13-dihydroxypropyl DDSQ with *S,S'*-bis(α,α'-dimethyl-α''-propargylacetate)trithiocarbonate (BDPT) was performed to obtain the macromolecular chain transfer agent (denoted DDSQ-CTA). Shown in Figure 1 are the ^{1}H NMR spectra of 3,13-dihydroxypropyl DDSQ, BDPT and DDSQ-CTA. For 3,13-dihydroxypropyl DDSQ, the signal of resonance at 0.32 ppm is assignable to the protons of methyl groups connected to the vertex silicon atoms of DDSQ. The signals of resonance at 0.74, 1.64 and 3.48 ppm are assignable to the protons of methylene groups of 3-hydroxylpropyl groups connected to the vertex silicon atoms and the resonance in the range of 7 ~ 8 ppm are attributable to the protons of aromatic rings. For BDPT, the intense single peak at 1.88 ppm is

assignable to the protons of methyl groups. With occurrence of the esterification, the peak of the methylene protons connected to hydroxyl groups in the difunctional POSS macromer was observed fully to shift to lower field at δ=3.96 ppm whereas other signals characteristic of 3,13-dihydroxypropyl DDSQ and BDPT remained invariant. The ^{1}H NMR spectroscopy indicates that the reacted product combined the structural features from 3,13-dihydroxypropyl DDSQ and BDPT. The DDSQ-CTA was subjected to gel permeation chromatography (GPC) to measure its molecular weight and its GPC curve was shown in Figure 2. The molecular weight was measured to be M_n=7,700 Da. Notably, the GPC curve exhibited the broad distribution of molecular weight with the value of M_w/M_n as high as 1.74. The results of the polymerization could be related to the higher steric hindrance of the reactions between 3,13-dihydroxypropyl DDSQ and BDPT, which resulted that the step-growth polymerizations were not easy to grow into the higher-molecular-weight species [34, 36]. Nonetheless, the results of ^{1}H NMR and GPC indicate that the DDSQ-CTA was successfully obtained.

Synthesis of Bead-like PNIPAAm Copolymers

The above DDSQ-CTA was used as the macromolecular chain transfer agent to mediate the radical polymerization of NIPAAm. With the RAFT polymerization, NIPAAm strucrual units would be inserted into the main chains between two adjecent DDSQ, *i.e.,* the bead-like PNIPAAm copolymers with DDSQ in the main chains were obtained. The content of DDSQ in the main chains was controlled according to the mass ratios of the DDSQ-CTA to NIPAAm and the conversion of NIPAAm monomer. Representatively shown in Figure 2A is the ^{1}H NMR spectrum of DDSQ3-PNIPAAm7. For comparison, the ^{1}H NMR spectra of DDSQ-CTA and plain PNIPAAm were also incorporated into this figure. Besides the signals of the protons assignable to PNIPAAm chain, the signals of the protons assignable to DDSQ were detected at 0.29, 0.70, 1.65 and 7.0 ~ 8.0 ppm; they were attributable to the protons of methylene groups connected to silicon atom, methylene of 3-isobutylpropyl groups, methyl of isobutyl groups and phenyl groups connected to vertex silicon atoms of DDSQ. The ^{13}C NMR spectrum of this polymer is shown in Figure 2B. The DDSQ structural units were characterized with the signals of ^{13}C resonance at 128, 130 and

134 ppm, assignable to the nucleus of carbons of aromatic rings and those at 1.1, 19.0, 100 ppm, attributable to the carbon nucleus of methyl and 3-oxylpropyl groups connected to the vertex silicon atom of DDSQ. The signals of resonance at 22.5, 41.2 and 42.2 were ascribed to the carbons of PNIPAAm structural units as indicated in this figure. The ^{1}H and ^{13}C NMR spectroscopy indicates that this polymer combined the structural features from DDSQ and PNIPAAm. All the organic-inorganic hybrid copolymers were subjected to gel permeation chromatography (GPC) to measure their molecular weights. The curves of GPC are presented in Figure 3 and the results of the RAFT polymerization are summarized in Table 1. It is noteworthy that all the GPC curves of the bead-like PNIPAAm samples displayed unimodal distribution of molecular weights although DDSQ-CTA displayed the multimodal distribution of molecular weight (See Figure 2). The appearance of unimodal distribution of molecular weights was readily accounted for the occurrence of RAFT polymerization. It is proposed that the living nature of RAFT polymerization originates from the reversible exchange between different propagating radicals (Pm• and Pn•) through an intermediate radical (**R**) process [69-72] as shown in Scheme 3. In the process of polymerization, the frequent exchange of the growing chain radicals (Pm• and Pn•) resulted in the homogenization of the chain lengths. As a result, the unimodal distribution of molecular weights was exhibited. Notably, the polydispersity indices (PDI) of all the bead-like PNIPAAm copolymers with DDSQ in the main chains were in the range of 1.26 ~1.70, which were higher than that of plain PNIPAAm. The values of PDI increased with increasing the content of DDSQ in the main chains. For instance, the PDI of DDSQ1-PNIPAAm9 was measured to be M_w/M_n=1.26 whereas that of DDSQ9-PNIPAAm1 to be M_w/M_n=1.70. The broadening of molecular weight distribution with increasing the content of DDSQ could be interpreted on the basis of the restriction of the POSS cases on the polymerization. In addition, this observation could be associated with the interaction between DDSQ and the GPC column much stronger than that between PNIPAAm chains and the GPC column. The results of ^{1}H NMR and GPC indicate that the bead-like PNIPAAm copolymers with DDSQ in the main chains were successfully obtained.

Glass Transition Temperatures (T_g's)

The bead-like PNIPAAm copolymers with DDSQ in the main chains were subjected to differential scanning calorimetry (DSC) and the DSC curves are shown in Figure 4. For comparison, plain PNIPAAm was also measured under the identical condition. The plain PNIPAAm displayed the glass transition temperature (T_g) at 144 ^oC. In the experimental range of temperature, all the bead-like PNIPAAm copolymers displayed single glass transitions. It should be pointed out that the single glass transitions did not purport the homogeneity of the bead-like PNIPAAm copolymers since the T_g of POSS could be too high to be detected. The observed glass transition is only ascribed to PNIPAAm chains in the bead-like PNIPAAm copolymers. Notably, the T_g's of the bead-like PNIPAAm copolymers were significantly lower than that of plain PNIPAAm; the T_g's decreased with increasing the content of DDSQ. It is proposed that the following three factors tendencies could affect the T_g's of the bead-like PNIPAAm copolymers. Firstly, the POSS cages in the main chains of the copolymers would restrict the motion of PNIPAAm segments, *i.e.,* the nanoreinforcement of POSS cages would give rise to the enhanced T_g's of PNIPAAm microdomains as reported in ample literature[2-6]. Secondly, the incorporation of the bulky POSS cages into the main chains simultaneously resulted in the increase in free volume in the copolymers. The introduction of bulky and vacant cage-like structure of POSS macromer in place of NIPAAm structural units could cause that the PNIPAAm chains were unable densely to pack in the glassy state, *i.e.,* the free volume in the polymers was significantly increased. As a consequence, the T_g's of the copolymers were depressed and decreased with increasing the content of DDSQ in the main chains. Thirdly, the lower T_g's for the bead-like copolymers with the higher contents of DDSQ could be associated with their relatively lower molecular weights. Nonetheless, this could not be a dominant factor for the bead-like copolymers with the molecular weights of M_n=10,500 Da or higher. It is proposed that the T_g's of PNIPAAm microdomains reflected the combined contributions from the above factors.

Self-assembly Behavior

The morphologies of the bead-like PNIPAAm copolymers with DDSQ in the main chains were investigated by means of transmission electron microscopy (TEM).

Shown in Figure 5 are the TEM micrographs of DDSQ1-PNIPAAm9, DDSQ3-PNIPAAm7 and DDSQ5-PNIPAAm5. In all the cases, the organic-inorganic hybrids displayed microphase-separated morphologies. Depending on the content of DDSQ, the spherical microdomains with the size of 10 ~ 200 nm in diameter were dispersed in a continuous matrix. The spherical microdomains are assignable to the POSS aggregates *via* POSS-POSS interactions[73,74] whereas the continuous matrix to PNIPAAm. The formation of the microphase-separated morphologies is attributable to the immiscibility of the POSS cages with PNIPAAm chains.

Both hydrophilicity of PNIPAAm and hydrophobicity of POSS could endow the bead-like PNIPAAm copolymers with the amphiphilicity. As a consequence, the bead-like PNIPAAm copolymers would display the self-assembly behavior in aqueous solution. In this work, the self-assembly behavior was investigated by means of transmission electron microscopy (TEM) and dynamic light scattering (DLS). The aqueous suspensions were used to prepare the specimens for TEM measurements *via* freeze-drying approach. Shown in Figure 6 are the TEM micrographs of the self-assembly nanoobjects from DDSQ1-PNIPAAm9, DDSQ3-PNIPAAm7 and DDSQ5-PNIPAAm5. For DDSQ1-PNIPAAm9, the spherical micelles with the size of *c.a.* 50 nm in diameter were formed (Figure 6A). It is proposed that the spherical micelles are composed of the POSS cores and PNIPAAm coronas. The POSS cores resulted from the POSS aggregates *via* POSS-POSS interactions[73,74]. With increasing the content of DDSQ in the main chains, the number of the spherical nanoobjects increased whereas the sizes remained almost invariant (See Figure 6B). While the content of DDSQ was increased up to 38 wt% (*i.e.*, for DDSQ5-PNIPAAm5) or higher, some vesicular nanoobjects with the size of about 100 nm in diameter appeared (See Figure 6C). It is proposed that the walls of the vesicular nanoobjects possessed a sandwich-like structure, in which the outer layers was comprised of PNIPAAm corona whereas the central layer was composed of the POSS aggregates *via* POSS-POSS interactions. The aqueous suspensions were further subjected to dynamic laser scattering to measure the size of the self-assembled nanoobjects. Shown in Figure 7 are the plots of hydrodynamic radius distribution as functions of hydrodynamic radius (R_h) for the suspebnsions of the bead-like PNIPAAm copolymers with DDSQ in the main chains at 24 ^oC. For DDSQ1-PNIPAAm9 and DDSQ3-PNIPAAm7, the unimodal distributions of intensity-averaged hydrodynamic

radius were exhibited with the R_h values of 167 and 221 nm, respectively. The sizes of the micelles increased with increasing the content of DDSQ. For DDSQ5-PNIPAAm5, a bimodal distribution of hydrodynamic radius was exhibited, with the R_h values of 62 and 253 nm, respectively. The DLS results were in good agreement with the morphological observation by means of TEM (See Figure 6B). The bimoldal distribution of hydrodynamic radius for DDSQ5-PNIOPAAm5 could correspond to the speherical and visecular nanoobjects, respectively. It is should be pointed out that the sizes of aggregates measured with TEM (Figure 7) are not necessarily identical with the R_h values by means of DLS. The former were obtained in the dry state and were much lower than the latter obtained in solutions, which contained the dominant contribution of the solvated coronas (*viz.* PNIPAAm).

Thermoresponsive Behavior

At low temperature, a single PNIPAAm chain adopts a random coil conformation in aqueous solution. Upon heating up to 32 ^{o}C or higher, the random coil collapses into a globule and become dehydrated. This coil-to-globule transition is the origin of the lower critical solution temperature (LCST) behavior of PNIPAAm in aqueous solution[17,19-29]. In the present case, each PNIPAAm chain was interlaid between two bulky and hydrophobic POSS cages. It is of interest to investigate the thermoresponsive behavior of PNIPAAm chains in the bead-like copolymers. In this work, the LCST behavior was investigated by means of micro-differential scanning calorimetry (Micro-DSC) and cloud-point analysis with UV-Vis spectroscopy. Shown in Figure 8 are the Micro-DSC curves of the aqueous suspensions of the bead-like PNIPAAm copolymers. For comparison, the DSC curve of plain PNIPAAm was also included. Plain PNIPAAm displayed a single exothermic transition at 32.3 ^{o}C. This exothermic peak stemmed from the coil-to-globule transition of PNIPAAm chains in aqueous solution and the temperature was thus determined as the LCST of PNIPAAm. For the bead-like PNIPAAm copolymers, the similar Micro-DSC curves were displayed, *i.e.,* the exothermic peaks were asymmetrical with steep leading regions before approaching the minima. Notably, the LCSTs of the organic-inorganic copolymers were significantly lower than plain PNIPAAm and decreased with increasing the content of DDSQ. For DDSQ5-PNIPAAm5, two separate exothermic

peaks were discernible. The decreased LCSTs for the bead-like PNIPAAm copolymers are ascribed to the inclusion of the hydrophobic component (*viz.* DDSQ), which significantly weakened the affinity of PNIPAAm chains with water molecules.

The LCST behavior was further investigated in terms of the cloud-point analysis by means of UV-Vis spectroscopy. Shown in Figure 9 are the plots of visible light (at λ=550) transmittance of the aqueous suspensions (0.2g/L) for the bead-like copolymers with DDSQ in the main chains as functions of temperature. For comparison, the curve of plain PNIPAAm aqueous solution was included. At the low temperature, the optical transmittances of all the aqueous solutions were higher than 85 %. Notably, the optical transmittances of the aqueous suspensions of the bead-like PNIPAAm copolymers were significantly lower than plain PNIPAAm. This observation is responsible for the formation of the self-assembled nanoobjects in the aqueous suspensions with considerable size. Upon heating to elevated temperatures, the optical transmittances were significantly decreased, indicating the occurrence of the LCST behavior. For plain PNIPAAm, the LCST was measured to be 32 ^{o}C and the transition range of temperature was as narrow as 2 ~ 3 ^{o}C; the optical transmittance was as low as 5.7 % after the coil-to-globule transition. Notably, the bead-like PNIPAAm copolymers displayed the features quite different from plain PNIPAAm. On the one hand, the LCSTs of the bead-like PNIPAAm copolymers were much lower than plain PNIPAAm; the LCSTs decreased with increasing the percentage of DDSQ in the main chains. This result was in good agreement with that of Micro-DSC. On the other hand, the coil-to-globule transitional ranges of the bead-like PNIPAAm copolymers were significantly broadened, especially for the copolymer with the higher content of DDSQ in the main chains (*e.g.*, DDSQ5-PNIPAAm5). The broadened ranges could be associated with the restriction of POSS cages on the coil-to-globule transition of PNIPAAm chains. It has been known that the bead-like PNIPAAm copolymers were self-assembled into the spherical or vesicular nanoobjects, in which PNIPAAm chains (*viz.* coronas) have to be densely attached onto the surface of the hydrophobic POSS aggregates. It is proposed that the conformational alteration of the PNIPAAm chains would be restricted by the hydrophobic POSS aggregates. As a consequence, the coli-to-globule transitional range was broadened. The higher the content of POSS in the bead-like PNIPAAm copolymers, the stronger the restriction was. In fact, we indeed observed that the

separate exothermic peaks in the Micro-DSC curve of DDSQ5-PNIPAAm5 (See Figure 8).

CONCLUSIONS

The bead-like PNIPAAm copolymers with DDSQ in the main chains were successfully synthesized *via* reversible addition-fragmentation chain transfer polymerization (RAFT). The macromolecular chain transfer agent was prepared *via* the polycondensation of 3,13-dihydroxypropyl DDSQ with *S,S'*-bis(α,α'-dimethyl-α''-propargylacetate)trithiocarbonate (BDPT). It was found that that the bead-like PNIPAAm copolymers with DDSQ in the main chains were microphase-separated. The interlay of the bulky POSS cages in the main chains of PNIPAAm affected the densely stacking of PNIPAAm chains and thus the glass transition temperatures (T_g) were significantly depressed. At lower content of DDSQ the bead-like PNIPAAm samples can be dispersed in aqueous solution and the copolymers were capable of self-organizing into different spherical and vesicular nanoobjects, depending on the content of DDSQ in the main chains. The results of micro-differential scanning calorimetry (Micro-DSC) and cloud point analysis with UV-vis spectroscopy showed that the thermoresponsive properties of the PNIPAAm chains in the bead-like PNIPAAm copolymers was still preserved while the content of DDSQ was lower than 50 mol %. Nonetheless, the POSS cages in the main chains exhibited the restriction of coil-to-globule transition of PNIPAAm chains.

ACKNOWLEDGMENT

The financial supports from Natural Science Foundation of China (No. 51133003 and 21274091) were gratefully acknowledged.

REFERENCES

1. M. G. Voronkov and V. I. Lavrent'yev, in *Inorganic Ring Systems*, Springer, 1982, pp. 199-236.
2. J. J. Schwab and J. D. Lichtenhan, 1998, *Appl. Organomet. Chem*., 1998, 12, 707-713.
3. G. Li, L. Wang, H. Ni and C. U. Pittman Jr, *J. Inorg. Organomet. Polym.*, 2001, 11, 123-154.
4. Y. Abe and T. Gunji, *Prog. Polym. Sci.*, 2004, 29, 149-182.
5. P. Lickiss and F. Rataboul, *Adv. Organomet. Chem*, 2008, 57, 1-116.
6. S.-W. Kuo and F.-C. Chang, *Prog. Polym. Sci.*, 2011, 36, 1649-1696.
7. B.-S. Kim and P. T. Mather, *Macromolecules*, 2002, 35, 8378-8384.
8. B.-S. Kim and P. T. Mather, *Macromolecules*, 2006, 39, 9253-9260.
9. B.-S. Kim and P. T. Mather, *Polymer*, 2006, 47, 6202-6207.
10. Y. Ni and S. Zheng, *Macromolecules*, 2007, 40, 7009-7018.
11. K. Zeng and S. Zheng, *J. Phys. Chem. B*, 2007, 111, 13919-13928.
12. K. Zeng, Y. Fang and S. Zheng, *J. Polym. Sci. Part B: Polym. Phys.*, 2009, 47, 504-516.
13. W. Zhang and A. H. Müller, *Macromolecules*, 2010, 43, 3148-3152.
14. K. Zeng, L. Wang and S. Zheng, *J. Colloid Interface Sci.*, 2011, 363, 250-260.
15. J. Choi, S. G. Kim and R. M. Laine, *Macromolecules*, 2004, 37, 99-109.
16. J. Choi, J. Harcup, A. F. Yee, Q. Zhu and R. M. Laine, *J. Am. Chem. Soc.*, 2001, 123, 11420-11430.
17. J.-C. Huang, C.-b. He, Y. Xiao, K. Y. Mya, J. Dai and Y. P. Siow, *Polymer*, 2003, 44, 4491-4499.
18. H. Liu and S. Zheng, *Macromol. Rapid Commun.*, 2005, 26, 196-200.
19. D. Neumann, M. Fisher, L. Tran and J. G. Matisons, *J. Am. Chem. Soc.*, 2002, 124, 13998-13999.
20. Y. Liu, Y. Ni and S. Zheng, *Macromol. Chem. Phys.*, 2006, 207, 1842-1851.
21. R. O. Costa, W. L. Vasconcelos, R. Tamaki and R. M. Laine, *Macromolecules*,

2001, 34, 5398-5407.

22. Y. Ni, S. Zheng and K. Nie, *Polymer*, 2004, 45, 5557-5568.
23. R. M. Laine, J. Choi and I. Lee, *Adv. Mater.*, 2001, 13, 800-803.
24. J. Choi, A. F. Yee and R. M. Laine, *Macromolecules*, 2003, 36, 5666-5682.
25. J. Choi, R. Tamaki, S. G. Kim and R. M. Laine, *Chem. Mater.*, 2003, 15, 3365-3375.
26. J. Choi, A. F. Yee and R. M. Laine, *Macromolecules*, 2004, 37, 3267-3276.
27. Y. Liu, S. Zheng and K. Nie, *Polymer*, 2005, 46, 12016-12025.
28. Y. Liu and S. Zheng, *J. Polym. Sci. Part A: Polym. Chem.*, 2006, 44, 1168-1181.
29. K. Huang and S. Kuo, *Macromol. Chem. Phys.*, 2010, 211, 2301-2311.
30. K. Zeng, Y. Liu and S. Zheng, *Eur. Polym. J.*, 2008, 44, 3946-3956.
31. M. E. Wright, D. A. Schorzman, F. J. Feher and R.-Z. Jin, *Chem. Mater.*, 2003, 15, 264-268.
32. S. Wu, T. Hayakawa, R. Kikuchi, S. J. Grunzinger, M.-A. Kakimoto and H. Oikawa, *Macromolecules*, 2007, 40, 5698-5705.
33. K. Yoshida, K. Ito, H. Oikawa, M. Yamahiro, Y. Morimoto, K. Ohguma, K. Watanabe and N. Ootake, US Patent 20,040,068,074, 2004.
34. S. Wu, T. Hayakawa, M.-a. Kakimoto and H. Oikawa, *Macromolecules*, 2008, 41, 3481-3487.
35. M. A. Hoque, Y. Kakihana, S. Shinke and Y. Kawakami, *Macromolecules*, 2009, 42, 3309-3315.
36. L. Wang, C. Zhang and S. Zheng, *J. Mater. Chem.*, 2011, 21, 19344-19352.
37. K. Wei, L. Wang and S. Zheng, *Polym. Chem.*, 2013, 4, 1491-1501.
38. K. Wei, L. Wang and S. Zheng, *J. Polym. Sci. Part A: Polym. Chem.*, 2013, 51, 4221-4232.
39. M. Heskins and J. Guillet, *J. Macromol. Sci. Part A: Pure Appl. Chem.*, 1968, 2, 1441-1455.
40. P. Kujawa, F. Tanaka and F. M. Winnik, *Macromolecules*, 2006, 39, 3048-3055.

41. H. G. Schild, *Prog. Polym. Sci.*, 1992, 17, 163-249.
42. C. Wu and S. Zhou, *Macromolecules*, 1997, 30, 574-576.
43. P. Kujawa and F. M. Winnik, *Macromolecules*, 2001, 34, 4130-4135.
44. A. Kikuchi and T. Okano, *Prog. Polym. Sci.*, 2002, 27, 1165-1193.
45. E. S. Gil and S. M. Hudson, *Prog. Polym. Sci.*, 2004, 29, 1173-1222.
46. T. Hoare and R. Pelton, *Macromolecules*, 2007, 40, 670-678.
47. X.-Z. Zhang, X.-D. Xu, S.-X. Cheng and R.-X. Zhuo, *Soft Matter*, 2008, 4, 385-391.
48. Y. Hirokawa and T. Tanaka, *J. Chem. Phys.*, 1984, 81, 6379-6380.
49. E. Sato Matsuo and T. Tanaka, *J. Chem. Phys.*, 1988, 89, 1695-1703.
50. A. Suzuki and T. Tanaka, *Nature*, 1990, 346, 345-347.
51. K. Otake, H. Inomata, M. Konno and S. Saito, *Macromolecules*, 1990, 23, 283-289.
52. H. Inomata, S. Goto, K. Otake and S. Saito, *Langmuir*, 1992, 8, 687-690.
53. M. Shibayama, M. Morimoto and S. Nomura, *Macromolecules*, 1994, 27, 5060-5066.
54. Liang, P. C. Rieke, J. Liu, G. E. Fryxell, J. S. Young, M. H. Engelhard and K. L. Alford, *Langmuir*, 2000, 16, 8016-8023.
55. L. D. Taylor and L. D. Cerankowski, *J. Polym.Sci.: Polym. Chem. Ed.*, 1975, 13, 2551-2570.
56. B. Ray, Y. Isobe, K. Morioka, S. Habaue, Y. Okamoto, M. Kamigaito and M. Sawamoto, *Macromolecules*, 2003, 36, 543-545.
57. B. Ray, Y. Isobe, K. Matsumoto, S. Habaue, Y. Okamoto, M. Kamigaito and M. Sawamoto, *Macromolecules*, 2004, 37, 1702-1710.
58. R. Plummer, D. J. T. Hill and A. K. Whittaker, *Macromolecules*, 2006, 39, 8379-8388.
59. A. N. Nedelcheva, N. G. Vladimirov, C. P. Novakov and I. V. Berlinova, *J. Polym. Sci. Part A: Polym. Chem.*, 2004, 42, 5736-5744.
60. C. M. Schilli, M. Zhang, E. Rizzardo, S. H. Thang, Y. K. Chong, K. Edwards, G. Karlsson and A. H. E. Müller, *Macromolecules*, 2004, 37, 7861-7866.

61. Y. Wang and H. Morawetz, *Macromolecules*, 1989, 22, 164-167.
62. J. Shan, J. Chen, M. Nuopponen and H. Tenhu, *Langmuir*, 2004, 20, 4671-4676.
63. M. Nuopponen, J. Ojala and H. Tenhu, *Polymer*, 2004, 45, 3643-3650.
64. M. Seino, T. Hayakawa, Y. Ishida, M.-a. Kakimoto, K. Watanabe and H. Oikawa, *Macromolecules*, 2006, 39, 3473-3475.
65. J. T. Lai, D. Filla and R. Shea, *Macromolecules*, 2002, 35, 6754-6756.
66. H. Bouchékif and R. Narain, *J. Phys. Chem. B*, 2007, 111, 11120-11126.
67. M. Nuopponen, K. Kalliomäki, A. Laukkanen, S. Hietala and H. Tenhu, *J. Polym. Sci. Part A: Polym. Chem.*, 2008, 46, 38-46.
68. S. E. Kirkland, R. M. Hensarling, S. D. McConaughy, Y. Guo, W. L. Jarrett and C. L. McCormick, *Biomacromolecules*, 2007, 9, 481-486.
69. J. Chiefari, Y. K. Chong, F. Ercole, J. Krstina, T. P. T. Le, R. T. A. Mayadunne, G. F. Meijs, G. Moad, C. L. Moad, E. Rizzardo and S. H. Thang, *Macromolecules*, 1998, 31, 5559-5562.
70. D. G. Hawthorne, G. Moad, E. Rizzardo and S. H. Thang, *Macromolecules*, 1999, 32, 5457-5459.
71. A. Alberti, M. Benaglia, M. Laus, D. Macciantelli and K. Sparnacci, *Macromolecules*, 2003, 36, 736-740.
72. R. T. A. Mayadunne, J. Jeffery, G. Moad and E. Rizzardo, *Macromolecules*, 2003, 36, 1505-1513.
73. L. Matejka, A. Strachota, J. Pleštil, P. Whelan, M. Steinhart and M. Šlouf, *Macromolecules*, 2004, 37, 9449-9456.
74. A. Strachota, I. Kroutilová, J. Kovárová and L. Matejka, *Macromolecules*, 2004, 37, 9457-9464.
75. A. Lee, J. Xiao and F. J. Feher, *Macromolecules*, 2005, 38, 438-444.
76. K. Wei, L. Li, S. Zheng, G. Wang and Q. Liang, *Soft Matter*, 2014, 10, 383-394.

Table 1 Results of RAFT polymerization of PNIPAAm with DDSQ in the main chains

Sample	[DDSQ-CTA] : [NIPAAm] (wt)	DDSQ (wt%)	M_n (GPC)	M_w/M_n
PNIPAAm	0:10	0	30,100	1.24
DDSQ1-PNIPAAm9	1:9	7.6	72,900	1.26
DDSQ3-PNIPAAm7	3:7	22.8	55,100	1.30
DDSQ5-PNIPAAm5	5:5	38.0	34,600	1.43
DDSQ7-PNIPAAm3	7:3	53.2	22,900	1.58
DDSQ9-PNIPAAm1	9:1	68.4	14,700	1.70
DDSQ-CTA	10:0	76.0	7,700	1.74

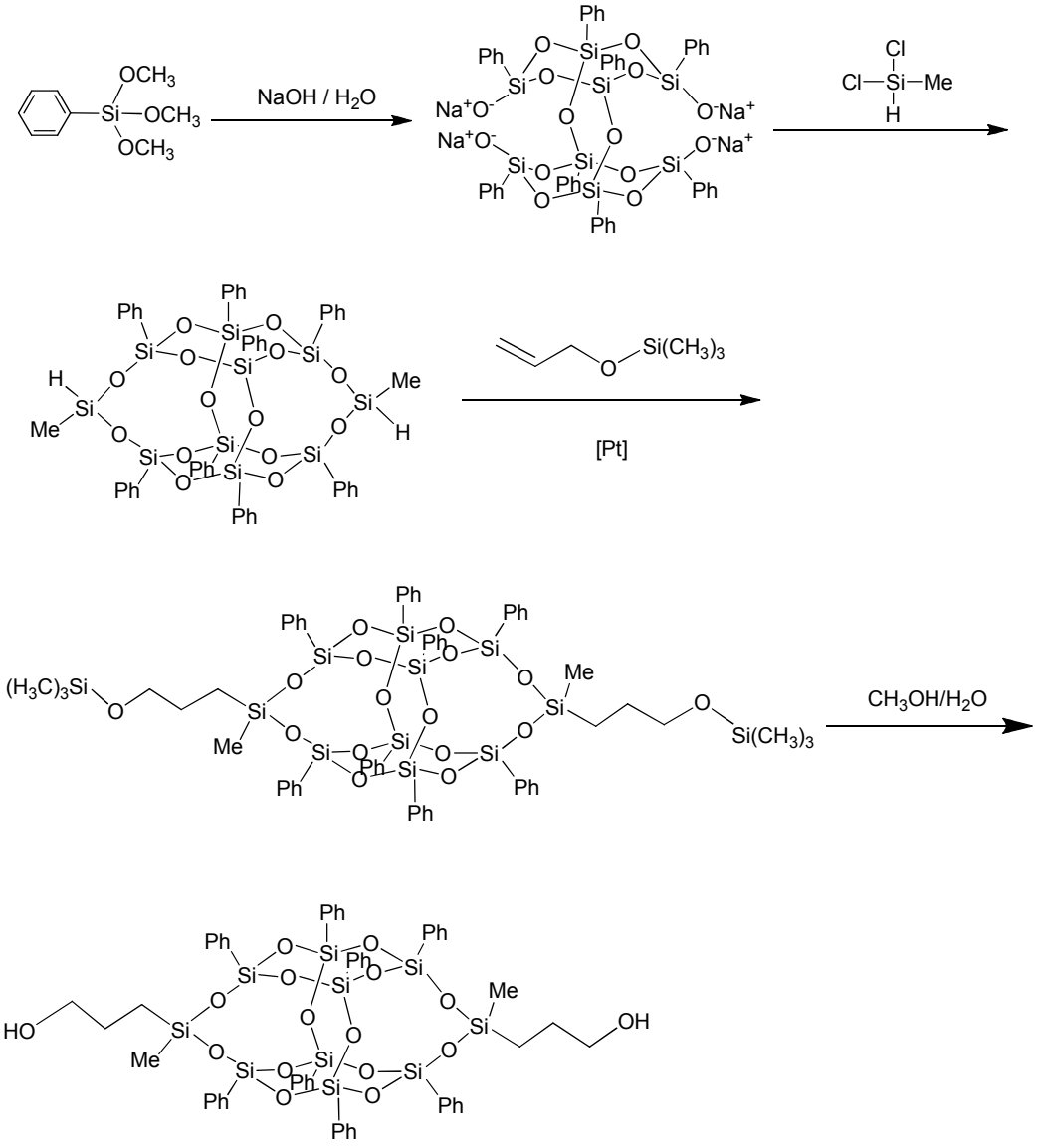

Scheme 1 Synthesis of 3,13-dihydroxyloctaphenyl DDSQ

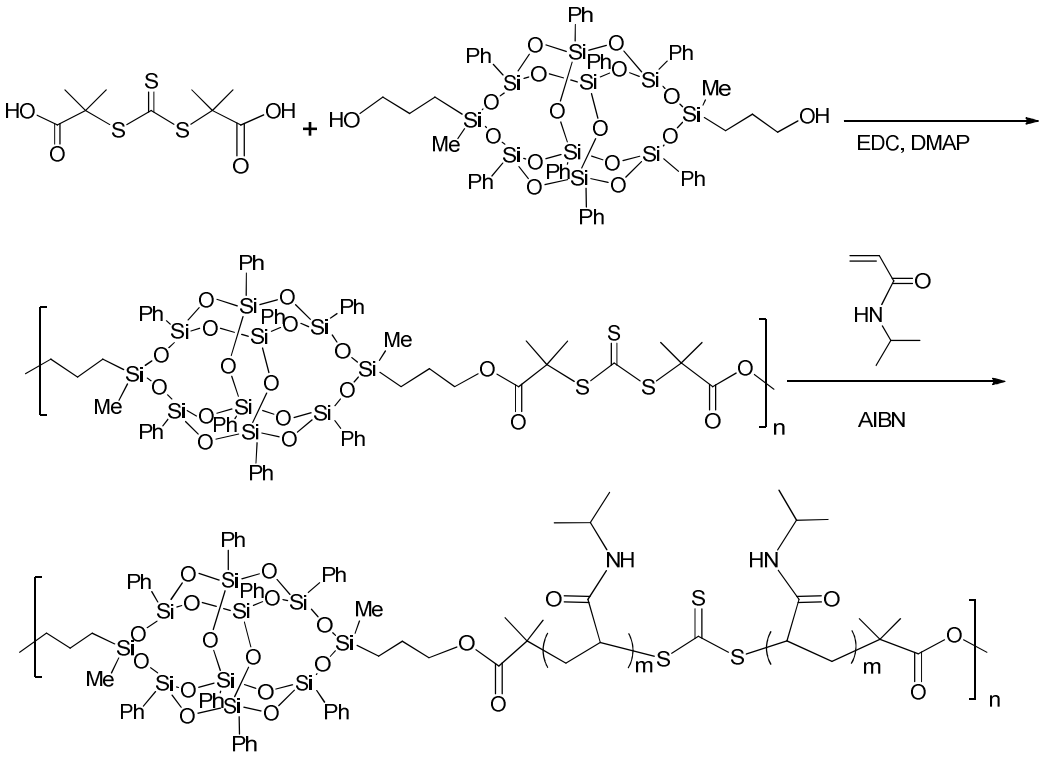

Scheme 2 Synthesis of bead-like PNIPAAm copolymers with DDSQ in the main chains

FIGURE CAPTIONS

Figure 1. ^{1}H NMR spectra of BDATC, DDSQ-CTA and 3,13-dihydroxypropyl DDSQ.

Figure 2. GPC curve of DDSQ-CTA copolymer, *i.e.,* the bead-like macromolecular chain transfer agent.

Figure 3. NMR spectra of DDSQ3-PNIPAAm7: A) ^{1}H spectrum and B) ^{13}C spectrum.

Figure 4. GPC curves of plain PNIPAAm and the bead-like PNIPAAm copolymers with DDSQ in the main chains.

Figure 5. DSC curves of plain PNIPAAm and the bead-like PNIPAAm copolymers with DDSQ in the main chains. A) PNIPAAm, B) DDSQ1-PNIPAAm9, C) DDSQ3-PNIPAAm7, D) DDSQ5-PNIPAAm5, E) DDSQ7-PNIPAAm3 and F) DDSQ9-PNIPAAm1.

Figure 6. TEM micrographs of the bead-like PNIPAAm copolymers with DDSQ in the main chains: A) DDSQ1-PNIPAAm9, B) DDSQ3-PNIPAAm5 and C) DDSQ5-PNIPAAm5.

Figure 7. TEM micrographs of the self-assembled nanoobjects of in aqueous solutions: A) DDSQ1-PNIPAAm9, B) DDSQ3-PNIPAAm7 and C) DDSQ5-PNIPAAm5.

Figure 8. Hydrodynamic radius of the self-assembled nanoobjects of the bead-like PNIPAAm copolymers with DDSQ copolymers in the main chains in the aqueous solutions at 25 ^{o}C.

Figure 9. Micro-DSC cures of pure PNIPAAm and the bead-like PNIPAAm with DDSQ in the main chains.

Figure 10. Plots of the transmission of the light (λ=550 nm) as functions of the temperature for the plain PNIPAAm and the bead-like PNIPAAm copolymers with DDSQ in the main chains solutions.

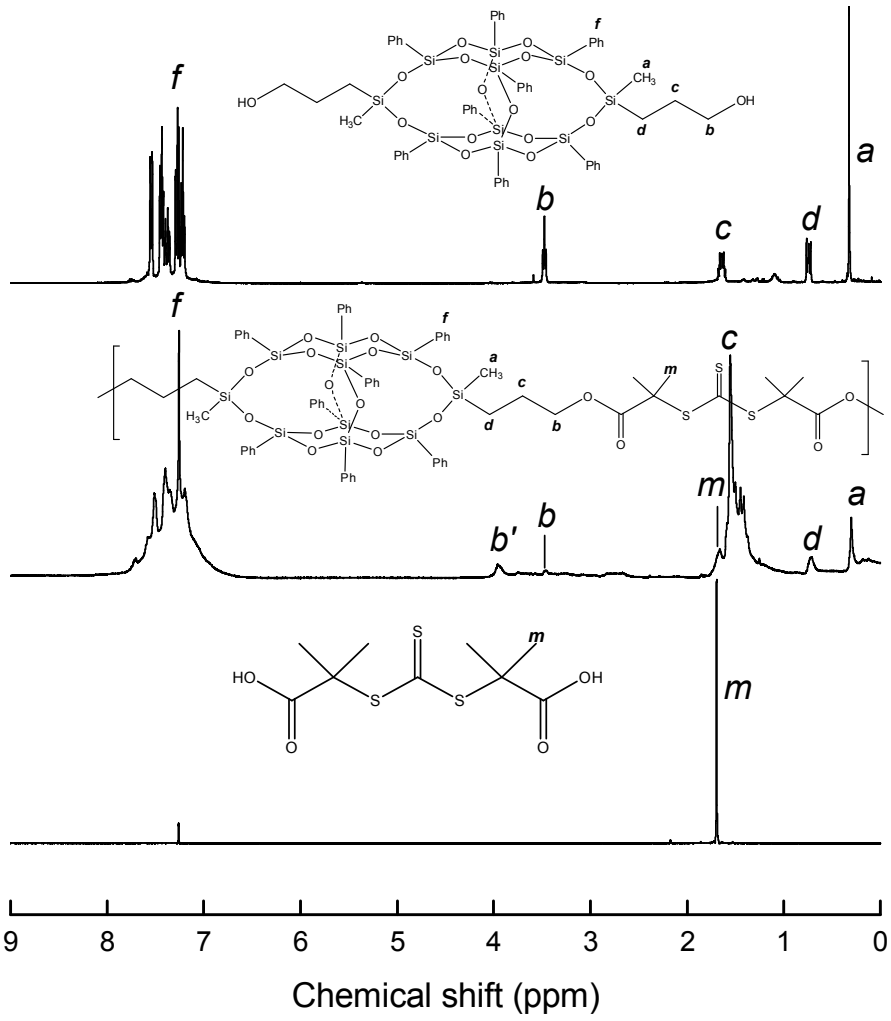

Figure 1

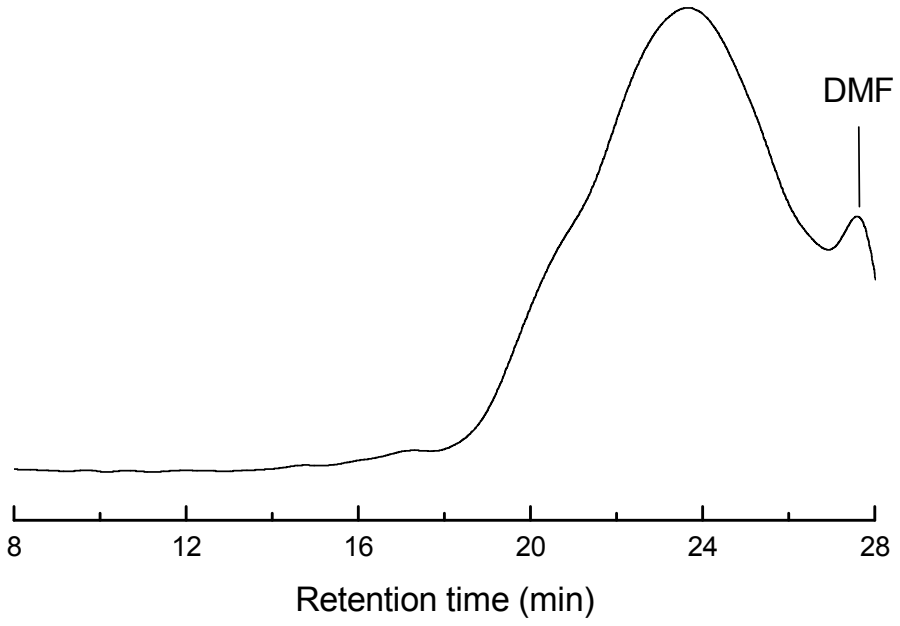

Figure 2

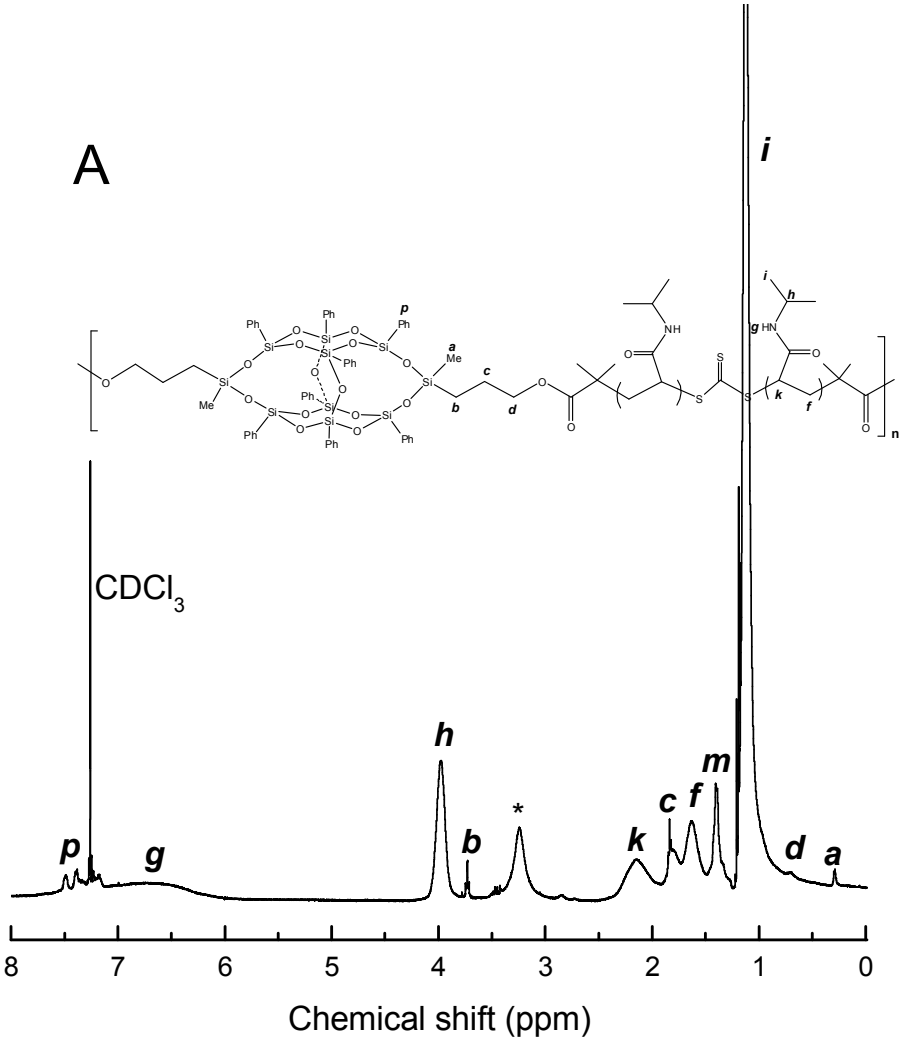
A
i
h
g
p
a
Me
c
b
d
k
f
n
CDCl3
h
m
c
f
*
p
g
b
k
d
a
8
7
6
5
4
3
2
1
0
Chemical shift (ppm)

Figure 3

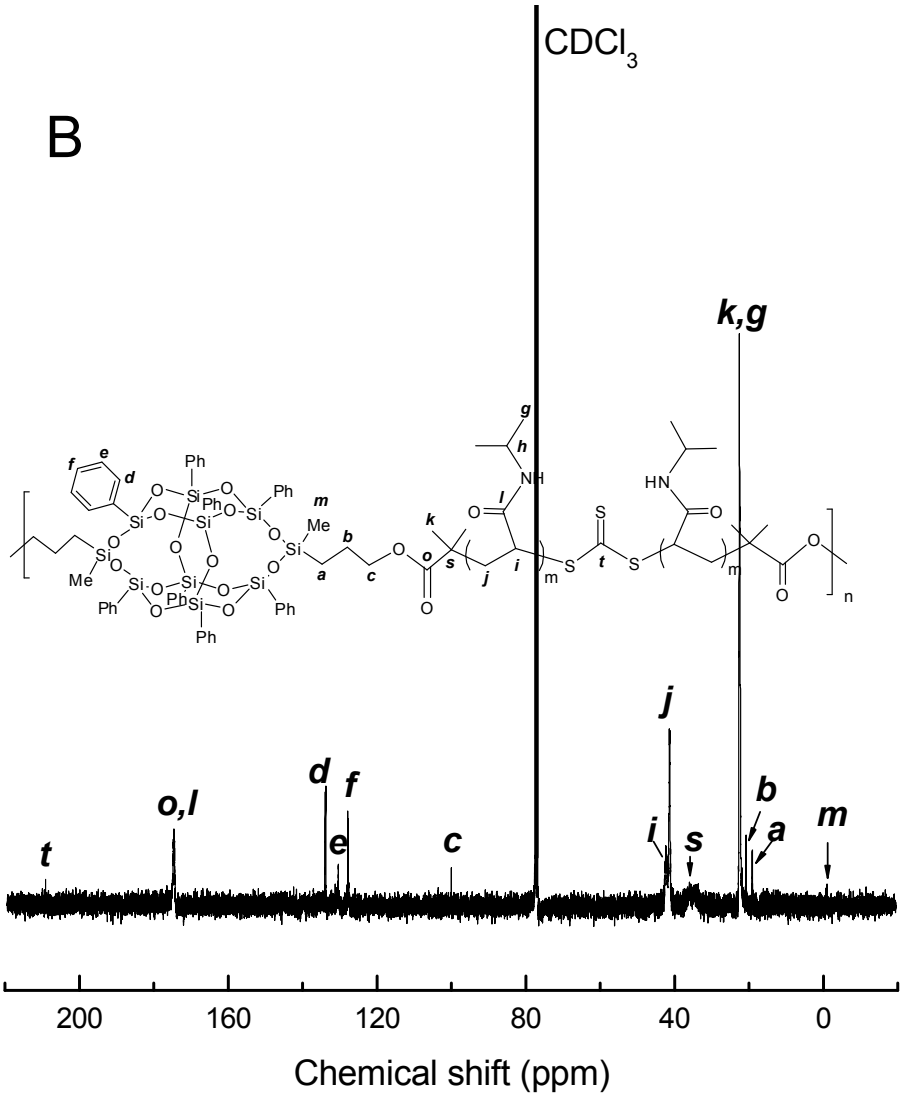

Figure 3 (*Continued*)

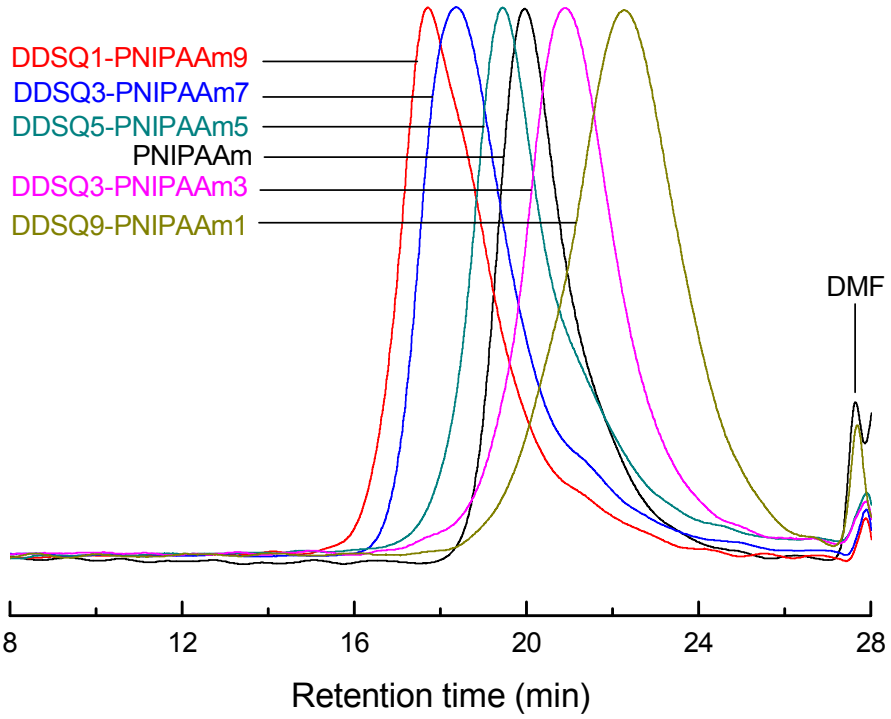
DDSQ1-PNIPAAm9
DDSQ3-PNIPAAm7
DDSQ5-PNIPAAm5
PNIPAAm
DDSQ3-PNIPAAm3
DDSQ9-PNIPAAm1
DMF
8
12
16
20
24
28
Retention time (min)

Figure 4

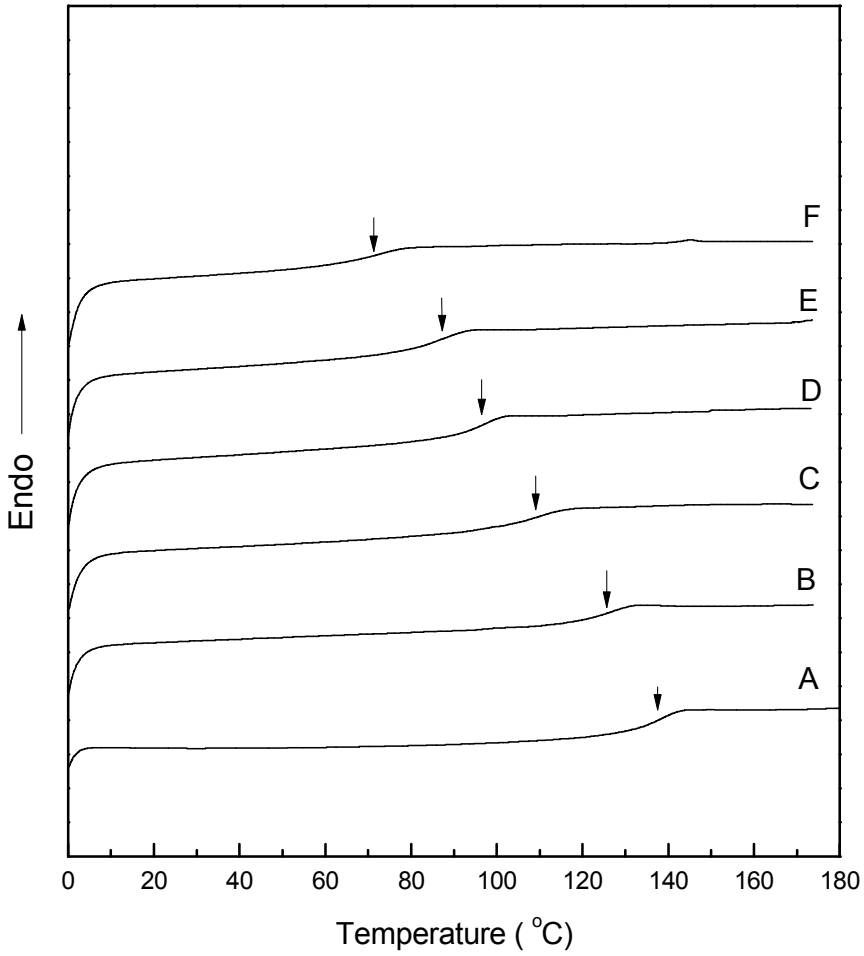

Figure 5

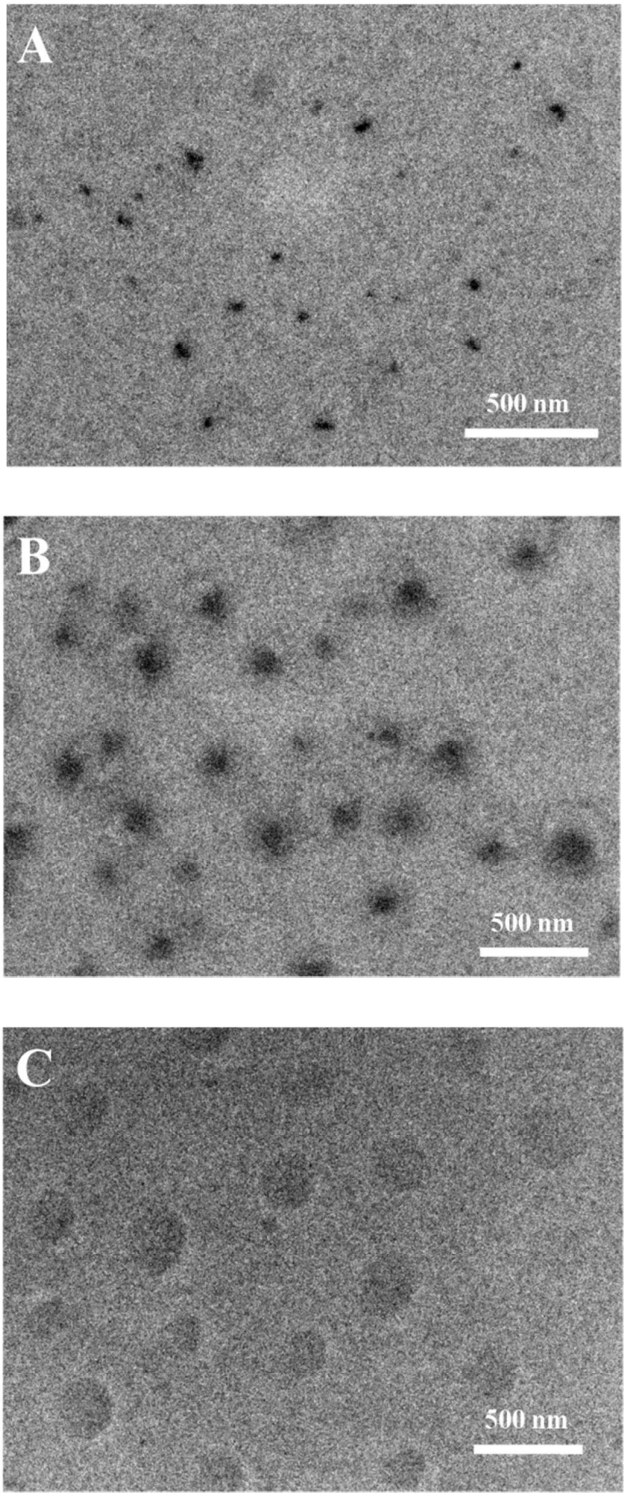

Figure 6

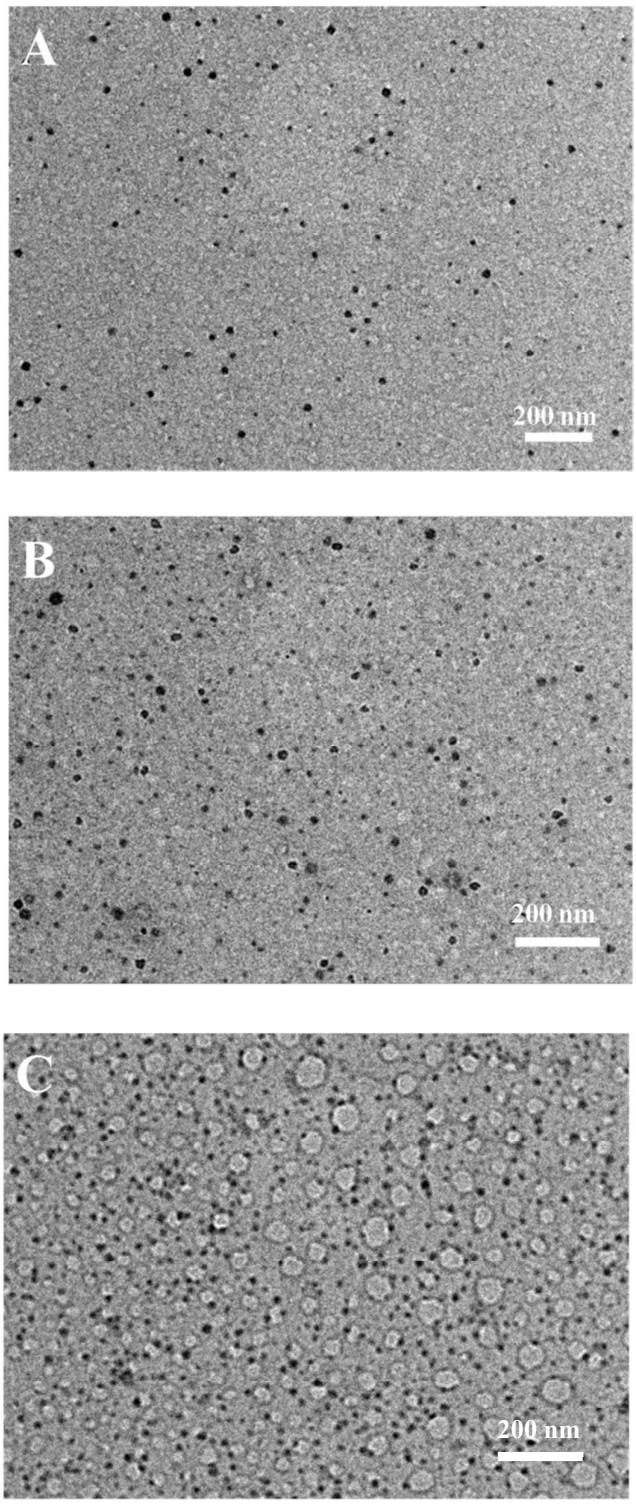

Figure 7

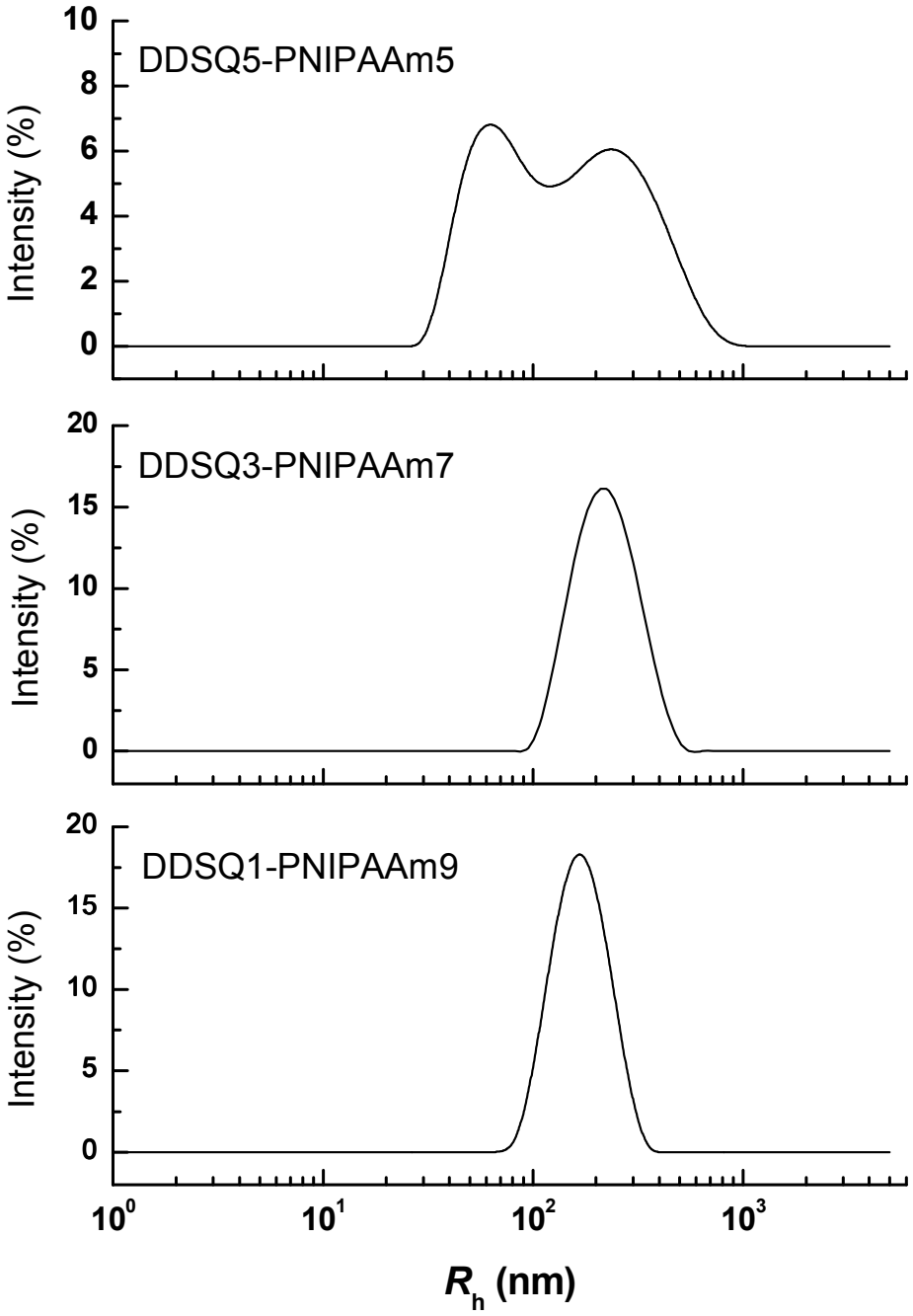
DDSQ5-PNIPAAm5
DDSQ3-PNIPAAm7
DDSQ1-PNIPAAm9
Intensity (%)
R_h (nm)

Figure 8

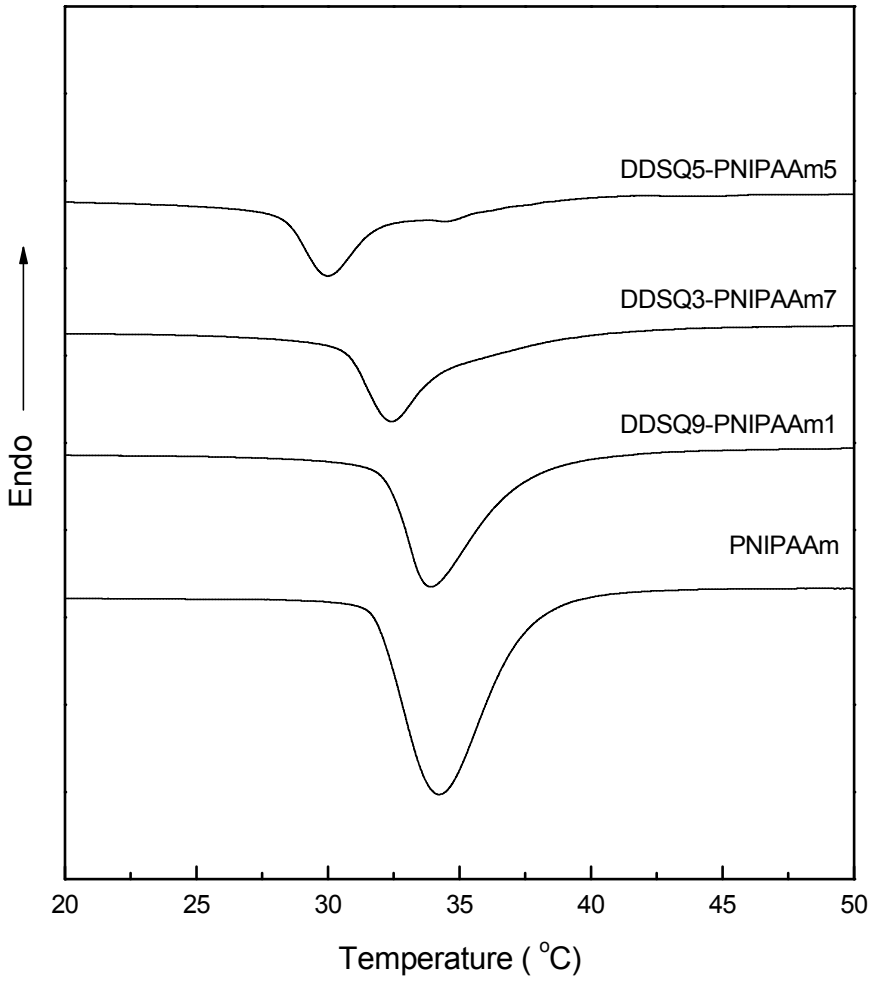
DDSQ5-PNIPAAm5
DDSQ3-PNIPAAm7
DDSQ9-PNIPAAm1
PNIPAAm
Endo
20
25
30
35
40
45
50
Temperature (°C)

Figure 9

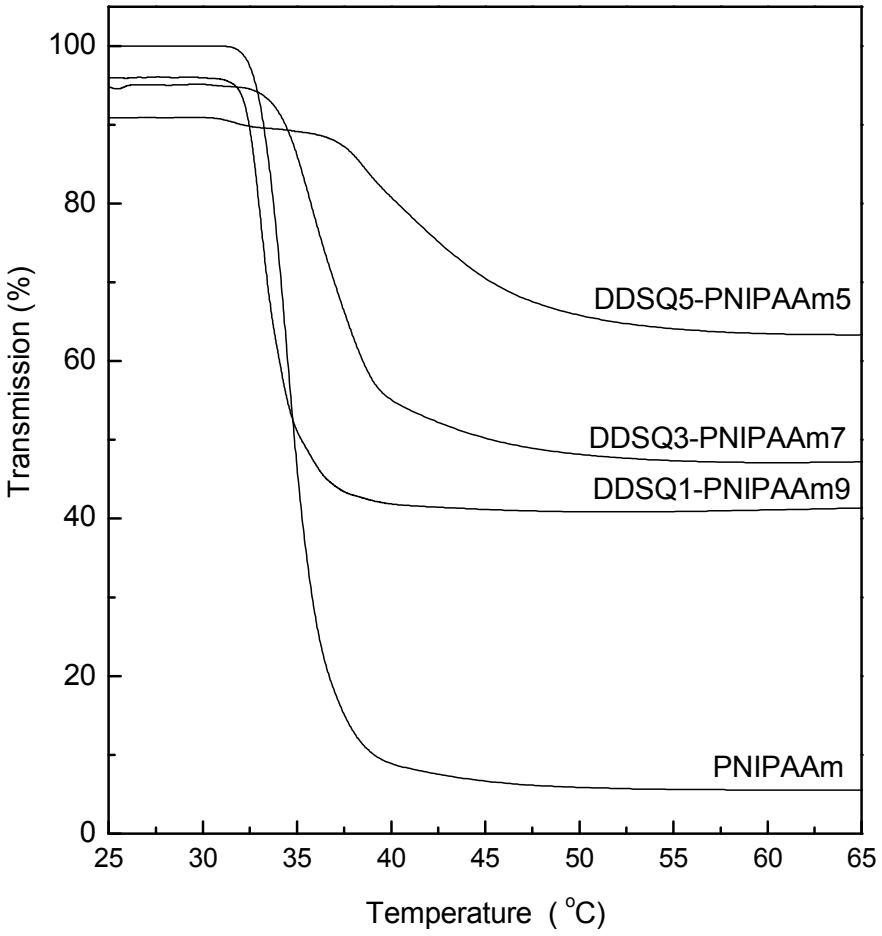
100
80
60
40
20
0
Transmission (%)
25
30
35
40
45
50
55
60
65
Temperature (°C)
DDSQ5-PNIPAAm5
DDSQ3-PNIPAAm7
DDSQ1-PNIPAAm9
PNIPAAm

Figure 10